Multistep Mechanism for the Devolatilization of Biomass Fast Pyrolysis Oils

Carmen Branca and Colomba Di Blasi*

Dipartimento di Ingegneria Chimica, Università degli Studi di Napoli "Federico II", P.le V. Tecchio, 80125 Napoli, Italy

Weight losses in air of four biomass fast pyrolysis oils (BTG, Dynamotive, Ensyn, Pyrovac), measured under controlled thermal conditions (heating rates of 5, 10, and 20 K/min up to 600 K), are used to formulate a multistep mechanism. This is based on the introduction of eight lumped classes of volatile products and a corresponding number of parallel reactions. The reaction rates are linear in the mass fractions of the lumped product groups and present the usual Arrhenius dependence on temperature. The simultaneous evaluation of all the measured curves produces the same set of activation energies (46, 65, 71, 80, 72, 84, 102, and 71 kJ/mol) and preexponential factors almost invariant with the bio-oil samples. In this way, the differences in the reactivity, deriving from the biomass properties and the pyrolysis characteristics, can be taken into account essentially by the stoichiometric coefficients. A relation is also provided between the eight lumped classes of products and the volatiles generated from evaporation and thermal cracking of bio-oil (permanent gases and 75 liquid compounds previously quantified).

Introduction

Renewable fuels, which can be easily stored and transported, are generated from biomass by means of a thermochemical conversion process indicated as pyrolysis. A proper selection of process conditions and feedstock properties allows different temperatures to be established during the thermal degradation of the organic components in biomass and high yields of solid[1] or liquid[2,3] products to be obtained. In particular, great interest has been addressed to liquid products (bio-oil, bio-crude, or pyrolyis liquid) because they have the potential to be used as a fuel oil substitute in many applications for heat or electricity generation.[4] Several companies have shown interest in using bio-oil, and results of experimental tests are available for furnaces, boilers, Diesel engines, gas turbines, and Stirling engines (see the reviews of refs 4 and 5). On the contrary, research activities carried out to understand the fundamentals of bio-oil combustion are only a few, and none of them examines the process kinetics.

The combustion of single bio-oil droplets[6−9] has shown a process dominated by a strong interaction between chemical and physical processes and consisting of several steps, which include evaporation, thermal cracking and polymerization of the bio-oil components, ignition, quiescent burning, droplet microexplosions, burning of droplet fragments, and formation and burnout of cenosphere particles (secondary char). Classical thermogravimetry[10,11] has also been applied, but the absence of accurate temperature control again hinders the analysis of the intrinsic reaction kinetics and reactivity of the samples. A method has been recently proposed by Branca et al.[12,13] to carry out weight loss measurements of bio-oil droplets in air under assigned thermal conditions and a kinetic control. The combustion process is investigated into two separate stages. The first, which foresees a final temperature of 600 K, concerns the devolatilization (evaporation/cracking) of the oil and secondary char formation, processes associated with sample swelling and solidification. After collection and milling, in the second stage, heterogeneous combustion of the secondary char is carried out up to temperatures of 873 K.

The combustion behavior of four bio-oils, derived from wood or bark by means of different fast pyrolysis technologies, has been studied using a single heating rate of 5 K/min.[13] The same qualitative features have been observed in all cases, but quantitative differences stem from both the different chemical composition, contents of solids and pyrolytic lignin. Secondary char formation and sample modification, which begin for temperatures of about 460−490 K, are also highly affected by physical properties, in particular viscosity. For the first stage, indicated as devolatilization, the main reaction zones have been identified which can be related to the dynamics of the bio-oil components. However, a reaction mechanism and the quantitative evaluation of the related kinetic constants are not yet available.

In this study, the experimental procedure developed by Branca et al.[12,13] is applied to measure weight loss curves during the devolatilization stage of bio-oils by varying the heating rate. This parameter is important to clarify the effects of temperature on the devolatilization process and to carry out a kinetic analysis. Indeed, the simultaneous evaluation of experimental data, obtained for different heating rates, is indicated as a means to avoid compensation effects[14] in the determination of the activation energies and preexponential factors of the reaction rates. The experimental measurements are then interpreted by a multistep devolatilization mechanism, the corresponding kinetic constants are estimated and a relation is provided between each reaction step and the bio-oil composition.

Experimental Details

The bio-oil samples examined are indicated by the name of the production process. They were produced in a rotating cone reactor (BTG, The Netherlands) and a bubbling fluid-bed reactor (Dynamotive, Canada) from softwood mixtures, in a transported bed reactor (Ensyn, Canada) from hardwood mixtures, and in a vacuum pyrolysis reactor (Pyrovac, Canada) from softwood barks. In accordance with fast pyrolysis conditions, reactor temperatures varied between 733 and 798 K, initial moisture contents between 7 and 12 wt % (dry basis), and particle sizes between 1 and 6 mm. Chemical[15,16] and physical[15] characterizations have also been carried out. These results, which are important for the kinetic analysis presented below, are summarized in Table 1 (yields and boiling temperatures of 75 species

* To whom correspondence should be addressed. Tel: 39-081-7682232. Fax: 39-081-2391800. E-mail: diblasi@unina.it.

10.1021/ie060161x CCC: $33.50
Published on Web 07/13/2006

Table 1. Yields and Boiling Temperatures of Bio-oil Compounds

compound	T_b (K)	BTG (wt %)	Dynamotive (wt %)	Ensyn (wt %)	Pyrovac (wt %)
formaldehyde	254	2.63	2.07	0.83	0.76
acetaldehyde	294	0.92	1.01	0.68	0.55
propionaldehyde	322	0.03	0.05	0.01	0.01
glycolic acid	323	0.57	0.50	0.31	1.07
glyoxal	324	1.51	1.32	0.84	0.92
acetone	329	0.12	0.15	0.15	0.14
methanol	338	0.91	1.03	0.39	0.07
2-oxobutanoic acid	351	0.18	0.17	0.13	0.15
ethanol	352	0.00	0.09	0.06	0.01
methyl ethyl ketone	353	0.20	0.37	0.06	0.23
2-propanol	356	0.25	0.37	0.00	0.06
(5*H*)-furan-2-one	360	0.54	0.62	0.50	0.51
water	373	30.40	21.10	20.30	15.70
formic acid	374	0.19	0.13	0.12	0.07
hydroxyacetaldehyde	383	6.65	5.65	3.69	2.54
5-hydroxymethylfurfural	388	0.49	0.52	0.23	0.83
acetic acid	391	3.17	2.46	4.73	2.25
butanol	391	3.15	2.85	1.29	0.80
lactic acid	395	0.21	0.18	0.09	0.08
4-propylguaiacol	399	0.07	0.14	0.07	0.05
4-acetonguaiacol	400	0.10	0.14	0.07	0.11
propionic acid	414	0.28	0.33	0.66	0.30
acrylic acid	412	0.14	0.03	0.04	0.08
hydroxypropanone	419	2.82	3.91	1.63	1.10
furantetrahydro-2,5-dimethoxy (cis)	419	0.03	0.05	0.00	0.00
furantetrahydro-2,5-dimethoxy (trans)	419	0.01	0.01	0.01	0.00
4-methylsyringol	419	0.13	0.12	0.22	0.15
isobutyric acid	427	0.07	0.19	0.06	0.18
furfuryl alcohol	430	0.07	0.08	0.08	0.09
3-methyl-2-cyclopentenone	431	0.11	0.16	0.23	0.21
2-methyl-2-cyclopentenone	431	0.06	0.17	0.14	0.53
2-ethyl-3-hydroxy-2-cyclopentene-1-one		0.04	0.04	0.04	0.09
2-hydroxy-2-cyclopentene-1-one		0.30	0.46	0.06	0.10
2-hydroxy-1-methyl-1-cyclopentene-3-one		0.43	0.50	0.32	0.52
1-hydroxy-2-butanone	433	0.07	0.21	0.09	0.10
2-furaldehyde	435	0.35	0.53	0.53	0.30
methacrylic acid	436	0.01	0.01	0.01	0.01
N-butyric acid	436	1.08	0.98	0.93	1.43
2-acetylfuran	446	0.03	0.03	0.05	0.03
acetoxyacetone	447	0.15	0.22	0.22	0.11
coniferylaldehyde	448	0.35	0.36	0.09	0.08
phenol	455	0.08	0.10	0.23	0.32
crotonic acid	456	0.07	0.02	0.05	0.06
valeric acid	459	0.05	0.34	0.15	0.34
3-hydroxypropanoic acid	-	0.02	0.00	0.02	0.04
5-methyl-2-furaldehyde	460	0.06	0.15	0.08	0.12
o-cresol	464	0.02	0.04	0.08	0.13
syringaldehyde	466	0.04	0.00	1.16	0.07
tiglic acid	472	0.01	0.04	0.00	0.00
4-methylpentanoic acid	472	0.01	0.01	0.00	0.02
p-cresol	475	0.02	0.04	0.05	0.12
m-cresol	475	0.01	0.03	0.04	0.10
hexanoic acid	477	0.05	0.14	0.16	0.16
2-ethylphenol	478	0.00	0.00	0.01	0.02
guaiacol	478	0.36	0.53	0.21	0.33
2,5- + 2,4-dimethylphenol	484	0.02	0.05	0.07	0.22
4-hydroxybenzaldehyde	490	0.01	0.01	0.01	0.03
4-methylguaiacol	494	0.65	1.23	0.23	0.41
vinylguaiacol	497	0.10	0.13	0.00	0.07
3,4-dimethylphenol	500	0.00	0.01	0.01	0.02
4-ethylguaiacol	508	0.12	0.37	0.08	0.13
2-methyl-4-propylphenol	513	0.02	0.09	0.01	0.03
1,2-benzendiol	518	0.00	0.13	0.10	0.91
levulic acid	519	0.12	0.11	0.11	0.23
benzoic acid	522	n.d.	0.02	0.00	0.05
eugenol	526	0.42	0.71	1.80	0.24
syringol	536	0.16	0.14	0.61	0.21
vanillin	539	0.82	0.29	0.08	0.25
isoeugenol (cis + trans)	541	1.41	2.80	0.49	1.18
acetosyringone		0.01	0.00	0.21	0.02
hydroquinone	558	0.17	0.30	0.33	0.47
levoglucosan	659	2.96	4.48	3.71	3.72
glucose		0.00	0.00	0.00	0.00
xilose		0.00	0.14	0.00	0.00
cellobiosan		1.80	2.30	0.00	0.70

Table 2. Main Physical Properties, Pyrolytic Lignin Contents, and Elemental Composition of the Bio-oil Samples

bio-oil	solid content (wt %)	viscosity × 10^3 (m^2/s) 293 K	viscosity × 10^3 (m^2/s) 313 K	pyrolytic lignin (wt %)	elemental analysis C (wt %)	H (wt %)	N (wt %)	O (wt %)
BTG	0.08	0.10	0.03	8	37.1	7.6	0.1	55.1
Dynamotive	0.10	0.03	0.01	25	44.7	7.2	0.1	48.1
Ensyn	0.43	1.27	0.21	54	47.2	6.9	0.1	45.6
Pyrovac	1.02	1.71	0.23	44	51.4	7.0	0.3	41.6

as in ref 13) and Table 2 (solid content, viscosity, content of pyrolytic lignin, and elemental analysis, as in ref 15), respectively.

Differences in the properties of the bio-oils are due to the pyrolysis reactor, the method of liquid collection, and feedstock properties, with the last two items playing the major role.[16] The entire amount of liquid collected was provided by BTG and Dynamotive and presumably by Ensyn whose collection method also included water scrubbing. For the Pyrovac technology, apart from the use of bark (versus wood), the liquid was collected into two fractions: a low-volatility organic fraction, which was provided for the analyses, and the water and volatile-rich fraction. In this case, much lower amounts of major carbohydrates and furans are observed. On the contrary, the yields of phenolics are roughly 2−4 times higher. In accordance with the different lignin structure, the yields of guiacols are higher for the softwood oils (BTG and Dynamotive samples), whereas the hardwood oils (Ensyn sample) show much higher contents of syringols. The solid content is relatively low in all cases, though it varies by about 1 order of magnitude between the BTG and Dynamotive samples, on one side, and the Ensyn and Pyrovac samples, on the other. The content of pyrolytic lignin and the viscosity are also much higher for the last two samples. It is plausible that these features together with the lower water content are responsible for the highest percent of carbon.

The thermogravimetric system, used to investigate the devolatilization behavior of bio-oils, is the same as in refs 12 and 13. It consists of a radiant heating chamber, a quartz reactor, a PID temperature controller, a gas feeding system, an acquisition data set, and a precision balance. The furnace is a radiant chamber, which creates a uniformly heated zone, where a quartz reactor is located while a proper reaction environment is established by a continuous air flow. The liquid is exposed to thermal radiation by means of a semispherical quartz cup. This is supported by Ni−Cr wires wrapped to steel rods and positioned at the center of the uniformly heated zone of the furnace. The steel support is connected to the balance for continuous weight loss measurements. To carry out a process under controlled thermal conditions, the intensity of the applied heat flux is used as the adjustable variable and the sample temperature is monitored. Following the differences between measured and desired temperature, the proportional-integral-derivative (PID) controller sends an electrical signal, *I*, which through a silicon-controlled rectifier (SCR) regulates the potential difference at the two ends of the furnace lamps. Temperature is measured by means of a thin chromel−alumel thermocouple.

The thermogravimetric program foresees a dynamic section, with heating rates of 5, 10, and 20 K/min from ambient conditions up to a temperature of 600 K and an isothermal section at 600 K (duration from about 60 to 30 min, depending on the heating rate). The isothermal part permits a complete devolatilization and avoids, at the same time, any significant activity of heterogeneous combustion reactions. The weight loss measurements have been carried out using samples consisting of 41 mg of liquid. Each test has been made in triplicate showing good repeatability. Changes in the sample mass (8−50 mg) do not result in any variation in the measured weight loss characteristics, indicating the absence of significant heat- and mass-transfer limitations. Therefore, the measured weight loss curves can be used for the analysis of the intrinsic kinetics of the process.

Kinetic Modeling

To interpret the integral and differential data measured for the weight loss of the four bio-oil samples, a devolatilization mechanism is proposed. This uses the same approach as that for the thermal decomposition of wood or biomass (for instance, refs 17−19), which assumes that the total volatiles released consist of *m* fractions, whose dynamics are described by first-order kinetics. Then, the overall mass loss rate is a linear combination of the single fraction rates. More specifically, the mechanism consists of *m* independent parallel reactions:

$$C_i \rightarrow V_i \qquad i = 1, m \qquad \text{(al−am)}$$

where C_i are assumed to be lumped groups of volatile species generated from the evaporation and the cracking reactions undergone by the bio-oil samples. A parallel-reaction mechanism (instead of a series reaction mechanism) is preferred because it is more flexible for taking into account the possible overlap between the devolatilization zones especially at high heating rates. The reaction rates present the usual Arrhenius dependence (A_i are the preexponential factors and E_i the activation energies) on temperature and are proportional to the mass fractions, Y_i, of components C_i:

$$R_i = A_i \exp(-E/RT)Y_i \qquad Y_i = 1, m$$

Because the sample temperature, *T*, is a known function of time ($T = T_0 + ht$; T_0 is the initial temperature, and *h* is the heating rate), the mathematical model consists of *m* ordinary differential equations for the mass fractions of the lumped classes of volatiles C_i:

$$\frac{\partial Y_i}{\partial t} = -R_i, \quad Y_i(0) = \nu_i, \qquad i = 1, m \qquad \text{(el−em)}$$

where ν_i, indicated in the following as stoichiometric coefficients, are the initial mass fractions of the lumped classes of volatiles generated.

The kinetic parameters are estimated through the numerical solution (implicit Euler method) of the mass conservation equations and the application of a direct method for the minimization of the objective function, which considers the integral (TG) and differential (DTG) data, following the method already described.[20] The simultaneous use of experimental data measured for variable heating rates avoids possible compensation effects in the kinetic parameters.[14] The parameters to be estimated are E_1-E_m, A_1-A_m, $\nu_1-\nu_m$, and *m* (a total of $3m + 1$ parameters). It should be noted that a pure devolatilization mechanism is proposed, and thus it does not describe secondary char formation. Indeed, given that a distinction is not possible between the already reacted and the still unreacted parts, the fractions of the solid residue generated from each devolatilization step cannot be measured. On the other hand, the devola-

Table 3. Estimated Values of the Preexponential Factors and Activation Energies for the First-Order Rates of the Parallel Reactions a1−a8 for the Four Bio-oil Samples

	reacn a_1	reacn a_2	reacn a_3	reacn a_4	reacn a_5	reacn a_6	reacn a_7	reacn a_8
				Preexponential Factor (s^{-1})				
BTG	9.00×10^4	9.54×10^6	1.50×10^7	4.33×10^7	4.80×10^5	1.34×10^6	1.10×10^7	2.60×10^3
Dynamotive	7.50×10^4	9.54×10^6	1.50×10^7	4.33×10^7	4.80×10^5	1.34×10^6	1.10×10^7	2.60×10^3
Ensyn	7.00×10^4	9.24×10^6	1.50×10^7	2.50×10^7	4.80×10^5	1.20×10^6	7.00×10^6	2.60×10^3
Pyrovac	7.00×10^4	1.44×10^7	1.70×10^7	4.80×10^7	3.90×10^5	8.00×10^5	7.40×10^6	2.60×10^3
				Activation Energy (kJ/mol)				
	46.5	64.7	71.0	80.3	72.0	84.4	102.0	71.3

tilization mechanism does not take into account the influence of temperature on the groups of reactions leading to volatile or solid (secondary char) formation. Hence, for each bio-oil sample, while the preexponential factors and activation energies are invariant, the stoichiometric coefficients can vary with the heating conditions, to describe the changes in the yield of solid residue with the heating rate. In other words, the reaction mechanism a1−a*m* can only predict the devolatilization rate, given the total amount of volatiles generated from the measured weight loss curves.

The deviation between measured and calculated curves is defined in accordance with previous analyses[18] as

$$\%\mathrm{dev}_{DTG} = \frac{\sqrt{S/N}}{(-\mathrm{d}Y/\mathrm{d}t_k)_{\mathrm{exp,peak}}} \times 100 \qquad (1)$$

$$S = \sum_{k=1,N} ((-\mathrm{d}Y/\mathrm{d}t_k)_{\mathrm{exp}} - (-\mathrm{d}Y/\mathrm{d}t_k)_{\mathrm{sim}})^2 \qquad (2)$$

where k represents the experimental (exp) or the simulated (sim) devolatilization rate at the time t (N is the number of experimental points (200 for the results discussed below) and the subscript peak indicates the maximum value). A deviation is similarly defined also for the integral data, $\%\mathrm{dev}_{TG}$.

The distributed activation energy model (DAEM), as already applied for the vapor-phase cracking of wood pyrolysis tars,[21] could also be used for the devolatilization of the bio-oil. However, the proposed kinetic model constituted by reactions a1−a*m* with first-order Arrhenius rates, provided a value of the parameter m is not exceedingly high, can be more easily coupled with the description of heat, mass, and momentum transfer in transport models. Some considerations should also be made in relation to the possible use of an evaporation model, as devolatilization of light liquid fuels is a purely physical process. However, as already reported,[12,13] the processes of bio-oil devolatilization consists of evaporation (at low temperatures) and evaporation combined with decomposition of the larger molecules (at higher temperatures). The wide range of volatility and the incomplete chemical characterization of bio-oil (about 300 species have been identified against the 75 quantified in Table 1) do not allow a detailed evaporation and cracking mechanism to be introduced. As for the application of first-order chemical reactions with an Arrhenius dependence on temperature for both evaporation and chemical release of volatile species, it is worth noting that even in the very simple case of moisture evaporation in wood, the same assumption has been used in several cases.[22−24] This allows for a finite thickness of the evaporating region and also eliminates the complications in the numerical solution, due to the presence of the unknown evaporation rate with an empirical expression for the vapor pressure, instead of an evolution equation or a simple production term.

Results and Discussion

To start the estimation procedure, using the measured data at the different heating rates, initial (guessed) values should be assigned for the model parameters. It is well-known that, given the chemical complexity of the bio-oil composition,[16] a very high number of chemical species is expected to be produced from the processes of evaporation and thermal cracking (the number of chemical species identified is on the order of 300). On the other hand, from the mathematical point of view, when a multistep process is fitted with a lumped reaction mechanism, the estimated activation energies are lower than the intrinsic (actual) values of each single step.[21] More specifically, in this study, the initial values of preexponential factors and activation energies are assigned on the analogy of the global mechanisms for the secondary reactions of tar vapors in pyrolysis reactors.[25] As for the number of reactions (and lumped classes of volatile products) a first set of simulations/estimations has been made using $m = 6$, in accordance with the number of main zones clearly shown by the measurements carried out at the slowest heating rate and extensively discussed by Branca et al.[13] However, this assumption gives poor predictions of the measured curves. Further calculations, made with $m = 7$, evidence an overestimation of the amount of volatiles released in correspondence with several peaks of the rate curves and, apart from the BTG sample, produce a fair description of the tail zone especially at slow heating rates. As a result of these preliminary evaluations, it was clear that at least eight reactions ($m = 8$) should be considered. Then, on the basis of this assumption, optimal values for the other parameters of the model have been determined.

The computations have been executed first for each sample by the simultaneous analysis of the curves measured for the three heating rates, by requiring that preexponential factors and activation energies remain invariant (as anticipated, for a devolatilization model, the stoichiometric coefficients should take into account the variations in the yields of volatile products generated as a consequence of the variations in the reaction temperature). The results of the computations show very close values of both activation energies and preexponential factors of the eight reactions for all the bio-oil samples. Therefore, as a final stage in the computational procedure, simultaneous evaluations have been made of the curves measured for the various samples, requiring that the activation energies of the eight reactions should be the same (preexponential factors and stoichiometric coefficients have been left free to vary for the different samples).

The results obtained for the model parameters are listed in Table 3 (activation energies and the preexponential factors) and Table 4 (stoichiometric coefficients), whereas the values of the parameters indicative of the goodness of the fitting, %dev, and the yields of secondary char, Y_c, are listed in Table 5. Comparison between measurements and predictions can be made through Figures 1−3 for the solid mass fractions and Figures 4−6 for the devolatilization rates at the various heating rates.

Table 4. Stoichiometric Coefficients of the Parallel Reactions a1−a8 for the Different Bio-oil Samples and Heating Rates

	ν_1	ν_2	ν_3	ν_4	ν_5	ν_6	ν_7	ν_8
				$h = 5$ K/min				
BTG	0.190	0.135	0.110	0.098	0.098	0.065	0.038	0.022
Dynamotive	0.095	0.108	0.087	0.096	0.107	0.114	0.046	0.048
Ensyn	0.031	0.070	0.118	0.076	0.080	0.110	0.102	0.050
Pyrovac	0.035	0.045	0.090	0.080	0.179	0.096	0.032	0.051
				$h = 10$ K/min				
BTG	0.165	0.134	0.112	0.092	0.087	0.092	0.038	0.039
Dynamotive	0.082	0.087	0.109	0.091	0.108	0.117	0.049	0.063
Ensyn	0.030	0.072	0.127	0.074	0.082	0.116	0.079	0.032
Pyrovac	0.038	0.039	0.073	0.078	0.185	0.091	0.077	0.053
				$h = 20$ K/min				
BTG	0.150	0.132	0.150	0.073	0.085	0.092	0.038	0.039
Dynamotive	0.082	0.077	0.110	0.080	0.118	0.130	0.050	0.064
Ensyn	0.025	0.080	0.150	0.073	0.082	0.095	0.079	0.022
Pyrovac	0.040	0.038	0.072	0.077	0.204	0.090	0.079	0.053

Table 5. Parameters Related to the Goodness of the Model Predictions for the Integral (TG) and Differential (DTG) Data for the Different Bio-oil Samples and Heating Rates

	heating rate = 5 K/min			heating rate = 10 K/min			heating rate = 20 K/min		
	$\%dev_{TG}$	$\%dev_{DTG}$	Y_c	$\%dev_{TG}$	$\%dev_{DTG}$	Y_c	$\%dev_{TG}$	$\%dev_{DTG}$	Y_c
BTG	0.399	4.550	0.244	0.341	1.763	0.241	0.212	1.232	0.241
Dynamotive	0.396	3.788	0.298	0.337	1.383	0.289	0.326	1.597	0.289
Ensyn	0.650	4.075	0.368	0.493	2.716	0.388	0.246	1.546	0.394
Pyrovac	0.367	5.261	0.392	0.141	2.858	0.366	0.484	1.692	0.347

As anticipated, the estimated activation energies are invariant for all the bio-oils and attain relatively low values (46.5, 64.7, 71.0, 80.3, 72.0, 84.4, 102.0, and 71.0 kJ/mol for the eight steps). Moreover, it can be observed that, apart from the first step, the preexponential factors are the same for the BTG and Dynamotive samples and limited to the third and fifth step for the Ensyn sample. The same values are also estimated for the first step of the Pyrovac and Ensyn samples. For the eighth step, the preexponential factor is always the same. Finally, for the remaining cases, the variations are small. It is plausible that these results can be attributed to the similarity in the lumped groups of species generated from the devolatilization process. Thus, the differences in the oil reactivity, deriving from both feedstock properties and pyrolysis conditions, can be taken into account essentially by the stoichiometric coefficients.

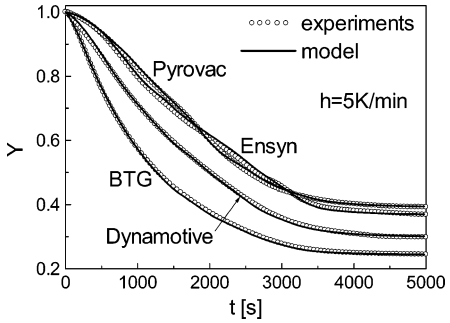

Figure 1. Weight loss (Y) curves of fast pyrolysis liquids as functions of time (dynamic section with a heating rate 5 K/min up to 600 K) as measured (symbols) and predicted by the model (lines).

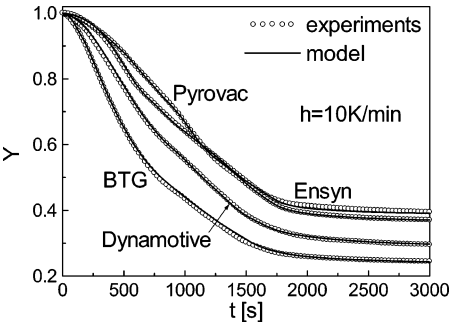

Figure 2. Weight loss (Y) curves of fast pyrolysis liquids as functions of time (dynamic section with a heating rate 10 K/min up to 600 K) as measured (symbols) and predicted by the model (lines).

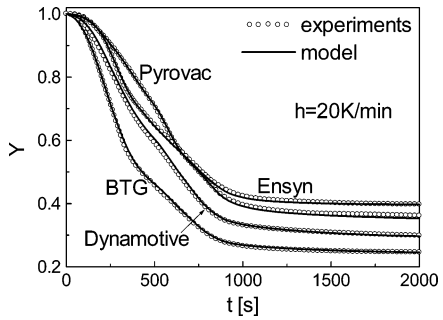

Figure 3. Weight loss (Y) curves of fast pyrolysis liquids as functions of time (dynamic section with a heating rate 20 K/min up to 600 K) as measured (symbols) and predicted by the model (lines).

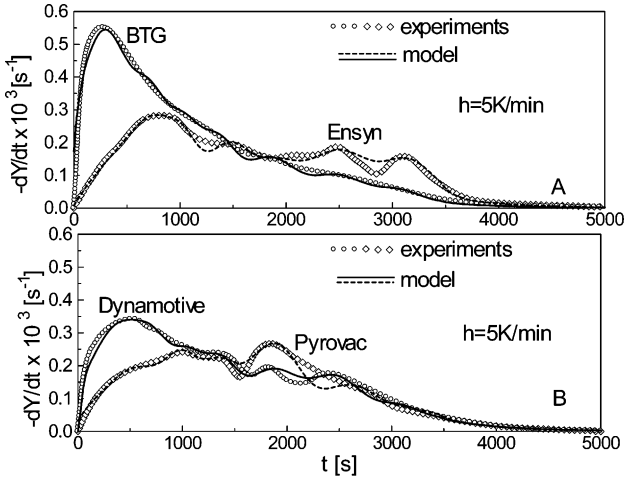

Figure 4. Weight loss rate ($-dY/dt$) curves of fast pyrolysis liquids as functions of time (dynamic section with a heating rate 5 K/min up to 600 K) as measured (symbols) and predicted by the model (lines): (A) BTG and Ensyn samples; (B) Dynamotive and Pyrovac samples.

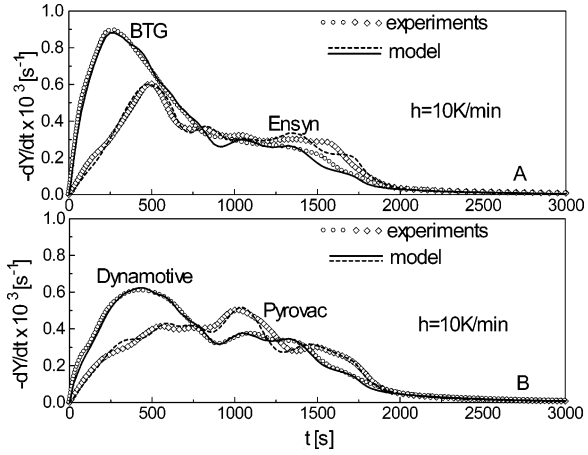

Figure 5. Weight loss rate ($-dY/dt$) curves of fast pyrolysis liquids as functions of time (dynamic section with a heating rate 10 K/min up to 600 K) as measured (symbols) and predicted by the model (lines): (A) BTG and Ensyn samples; (B) Dynamotive and Pyrovac samples.

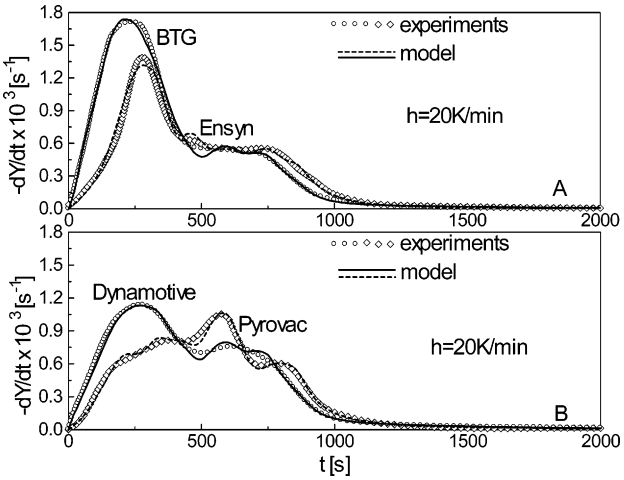

Figure 6. Weight loss rate ($-dY/dt$) curves of fast pyrolysis liquids as functions of time (dynamic section with a heating rate 20 K/min up to 600 K) as measured (symbols) and predicted by the model (lines): (A) BTG and Ensyn samples; (B) Dynamotive and Pyrovac samples.

The kinetic model proposed provides excellent or good agreement with the measurements. As expected, deviations are smaller for the integral data (Figures 1−3 and Table 5). The differential curves of bio-oil weight loss show complex dynamics, as already discussed[13] for a heating rate of 5 K/min. Several peaks and shoulders are present whose position and size are affected by the pyrolysis characteristics. In all cases, weight loss starts at low temperatures, given the presence of highly volatile compounds, and high rates are already attained at temperatures below 550 K. As the heating rate is increased, the qualitative features remain the same but peaks and shoulders tend to merge. As expected, the maximum devolatilization rates increase and the duration of the devolatilization process becomes shorter.

Differences between the yields of secondary char are quite high (Table 5) and reproduce the same trends as in the initial carbon content of the samples.[13] Given the relatively narrow range of values examined, the quantitative effects caused by the heating rates are small. However, it is important to note that secondary char yields decrease as the thermal conditions became more severe for the BTG, Dynamotive, and Pyrovac oils, whereas they become successively higher for the Ensyn oil. This peculiar behavior can be attributed to a higher activity of polymerization reactions, probably associated with the lower

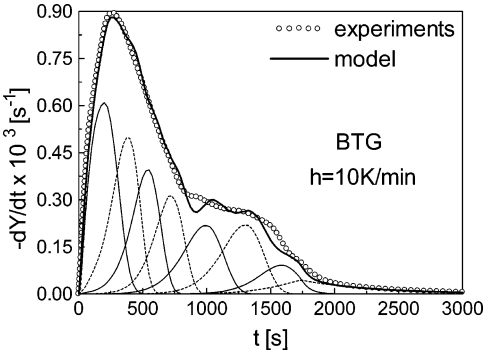

Figure 7. Predictions of the devolatilization rates of the eight lumped classes of volatile products (solid lines) and the total devolatilization rate (dashed line) for a heating rate of 10 K/min and the BTG oil (symbols represent the measured curve).

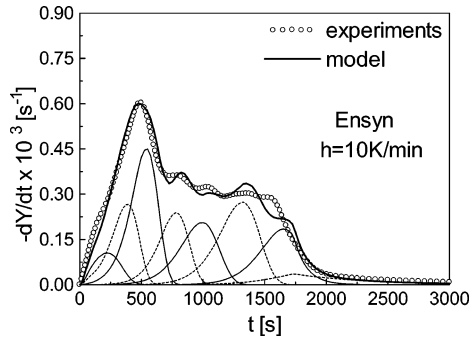

Figure 8. Predictions of the devolatilization rates of the eight lumped classes of volatile products (solid lines) and the total devolatilization rate (dashed line) for a heating rate of 10 K/min and the Dynamotive oil (symbols represent the measured curve).

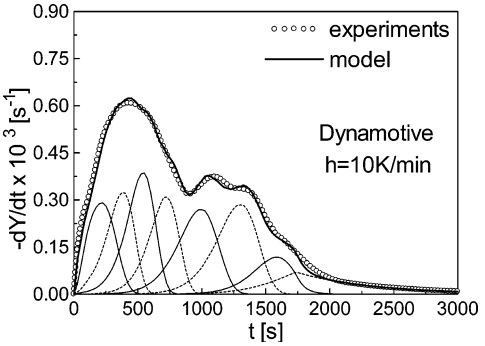

Figure 9. Predictions of the devolatilization rates of the eight lumped classes of volatile products (solid lines) and the total devolatilization rate (dashed line) for a heating rate of 10 K/min and the Ensyn oil (symbols represent the measured curve).

content of compounds showing boiling temperatures below 360 K (Table 1), compared with the other samples.

Further information on the process dynamics can be obtained from the time history of the component rates, reported in Figures 7−10, for the various oil samples and a heating rate of 10 K/min. In all cases, a significant overlap between the different reaction zones is seen, confirming the need of a parallel mechanism for the interpretation of thermogravimetric curves. The process dynamics remain qualitatively the same, as the heating rate is varied, but the amount of species released is slightly modified (Table 4) and the peak rates tend to become higher. The highest amount of volatiles is released in the first step (BTG, 19−15%), between the fifth and the sixth step (Dynamotive, 11−13%), in the third step (Ensyn, 12−15%), and in the fifth step (Pyrovac, 18−20.4%). In general, the reaction step associated with the highest amount of volatiles released also coincides with the

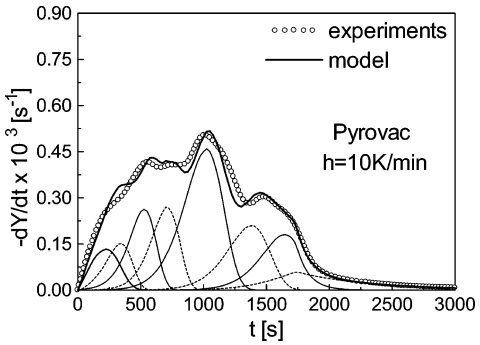

Figure 10. Predictions of the devolatilization rates of the eight lumped classes of volatile products (solid lines) and the total devolatilization rate (dashed line) for a heating rate of 10 K/min and the Pyrovac oil (symbols represent the measured curve).

attainment of the maximum devolatilization rate among the lumped classes of compounds (the Pyrovac and Ensyn oils for all the heating rates and the BTG oil for the heating rates of 5 and 10 K/min). The Dynamotive oil is an exception as the maximum devolatilization rates are always attained for relatively low temperatures (between the second and the third reaction step, depending on the heating conditions), but the highest yields of volatiles are released, with relatively slow rates, at higher temperatures over a wide time interval (for the BTG oil and a heating rate of 20 K/min the maximum devolatilization rate is attained by the third reaction; however the rate peaks of reactions a1−a3 are roughly the same). Examination of the component rates (Figures 7−10) and the stoichiometric coefficients (Table 4) reveals that a close similarity exists between the Ensyn and Pyrovac samples. A large part of the volatiles is released at low temperature in the case of the BTG sample, while an intermediate behavior is shown by the Dynamotive oil. The same considerations can also be made when looking at the values of the activation energies and preexponential factors presented above.

To give a physical basis to the mechanism a1−a8, an effort has been made to establish a relation between the reaction steps and the evaporation of the bio-oil compounds based on the corresponding boiling temperatures. For this purpose, considering the model predictions for a heating rate of 5 K/min, the temperature ranges have been evaluated corresponding to the release of the 60% of the total amount of volatiles involved with each reaction step (larger percentages and/or higher heating rates would not allow a sufficient separation to be achieved between the different devolatilization zones). The results are roughly the same for all the samples so that, using the quantified compounds and their boiling temperature (Table 1), the volatiles generated from each reaction can be identified. The volatile amounts computed in this way, α_{iev}, and those predicted by the model, α_i, expressed as percent of the initial sample mass, and the ranges of boiling temperatures of interest are listed in Table 6. It can be observed that, in all cases, model predictions for the reactions a1 and a2 are always higher or equal, whereas those of step a3 are much lower. It can be thought that water evaporation also contributes in the production of volatiles in the first and second steps. Indeed, the agreement between α_{iev}, and α_i becomes acceptable when the total amounts for the first three reactions are considered. Model predictions give higher figures for the reaction a4 (from about 20 to 40%) and especially for reactions from a5 to a7. It can be understood that, apart from the incomplete chemical characterization of the samples, for these reaction steps, thermal cracking significantly contributes in the devolatilization process with the formation of permanent gases. Finally, for the last step, differences are again reduced. On the basis of these considerations, the species involved with the eight steps of the proposed reaction mechanism a1−a8 can be detailed as in Figure 11.

A comparison can also be easily made with the eight-step devolatilizion mechanism proposed here and the conceptual reaction mechanism, comprising six main zones, previously introduced.[13] It appears that the first devolatilization zone

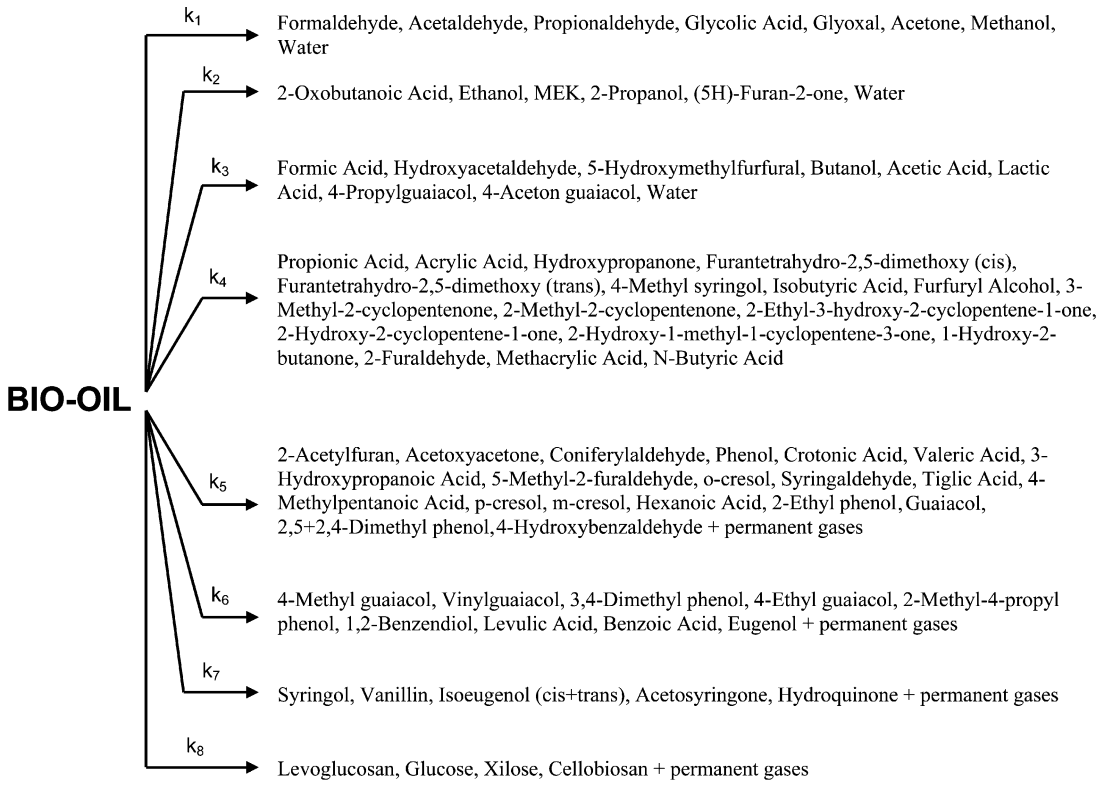

Figure 11. Reaction mechanism for bio-oil devolatilization with the indication of the chief compounds of the lumped classes of volatile products.

Table 6. Volatile Yields, Estimated According to the Boiling Temperatures of Liquid Compounds (Table 1), α_{iev}, and Predicted by the Model α_i, Expressed as Percent of the Initial Sample Mass, for the Reactions a1−a8 (the Interval of the Boiling Temperatures, ΔT_b, Evaluated from the Curves Simulated for a Heating Rate of 5 K/min When 60% of Each Amount of Volatiles Has Been Produced)

		BTG		Dynamotive		Ensyn		Pyrovac	
reaction	ΔT_b (K)	α_{iev} (%)	α_i (%)	α_{iev} (%)	α_i (%)	α_{iev} (%)	α_i (%)	α_{iev} (%)	α_i (%)
a_1	254−338	6.7	19.0	6.1	9.5	3.2	3.1	3.5	3.5
a_2	351−360	1.2	13.5	1.6	10.8	0.8	7.0	1.0	4.5
a_3	373−400	44.4	11.0	33.2	8.7	30.6	11.8	22.4	9.0
a_4	414−436	6.0	9.8	7.8	9.6	5.0	7.6	5.2	8.0
a_5	446−484	1.3	9.8	2.1	10.7	2.6	8.0	2.3	17.9
a_6	490−526	1.4	6.5	2.8	11.4	2.3	11.0	2.1	9.6
a_7	536−558	2.6	3.8	3.5	4.6	1.7	10.2	2.1	3.2
a_8	>580	4.8	2.2	6.9	4.8	3.7	5.0	4.4	5.1

(temperatures below 360 K) requires two devolatilization reactions (a1 and a2), whereas the second zone coincides with the third reaction a3. The boundaries for the third and fourth zones are slightly modified, and three reactions are needed for the description of the fifth and sixth zones.

Conclusions

An experimental method, previously developed, has been applied to investigate the devolatilization behavior of four bio-oils derived from wood/bark by means of different fast pyrolysis technologies (BTG, Dynamotive, Ensyn, and Pyrovac). A kinetic control has been established as the heating rate is varied (5, 10, and 20 K/min up to a final temperature of 600 K). The devolatilization rate curves show several peaks and shoulders, especially evident for the slowest heating rate, and quantitatively affected by the oil sample, that is, its specific chemical and physical properties. The process characteristics remain qualitatively the same as the heating rate is increased, but a large overlap occurs between the different reaction zones. The final yields of secondary char, significantly dependent on the nature of the oil, indicate that higher temperatures slightly enhance the reactions of thermal cracking (BTG, Dynamotive, and Pyrovac) or polymerization (Ensyn).

The measured curves are used to formulate a devolatilization mechanism based on the introduction of eight lumped classes of volatile products and a corresponding number of parallel reactions. The reaction rates are linear in the mass fractions of the lumped product groups and present the usual Arrhenius dependence on temperature. The simultaneous evaluation of the experimental data for the different bio-oils and thermal conditions has produced the same set of activation energies which, given the simplification introduced by the small number of reaction steps in comparison with the huge number of bio-oil compounds, are comprised within a range of relatively low values (46−102 kJ/mol). Preexponential factors are only slightly dependent on the bio-oil sample. In particular, except for the first reaction, the values are coincident for the BTG and Dynamotive samples and, for several steps, also for the Ensyn sample. Coincident values are also estimated, for some steps, for the Ensyn and Pyrovac samples. These results indicate that the devolatilization behavior of bio-oils is determined by the presence of lumped groups of species which are common to all the bio-oils examined. The different percentages and the changes in the devolatilization rate can be well described by variations in the stoichiometric coefficients. Indeed, after the evaluation of the temperature range, where each reaction is active, and using the current state of the art on bio-oil chemical characterization, the compounds of each lumped class of volatile products have been identified.

The first three reactions are associated with the evaporation of water and light compounds with boiling temperatures up to about 340 K (for instance, formaldehyde, acetaldehyde, acetone, and methanol), 360 K (for instance, ethanol, 2-propanol, and (5*H*)-furan-2-one), and 400 K (for instance, hydroxyacetaldehyde, acetic acid, and butanol). For higher temperatures, the reactions of thermal cracking, giving rise to the formation of permanent gases, become important. Furthermore, the evaporation is still important and corresponds to zones limited by a temperature of about 440 K (for instance, several acids, hydroxypropanone, and 2-furaldehyde), 490 K (light phenolic compounds), and 530 and 560 K (more complex phenols). Finally, the last step is probably related to the release of volatiles from sugars conversion.

The results of this study are particularly important for the application of biomass fast pyrolysis oils because, after the qualitative analysis carried out by this research group, a kinetic mechanism is provided for the first time. A quantitative evaluation is made available of the rate constants, free of compensation effects, applicable for different commercial technologies. Further research, however, is still needed for the heterogeneous combustion of the secondary char generated from the devolatilization of bio-oils.

Acknowledgment

The kindness of the bio-oil producers (BTG in The Netherlands and Dynamotive, Ensyn, and Pyrovac in Canada), who made samples available through the European network PyNe, is greatly appreciated. C.D.B. also thanks the PyNe group for many useful discussions on bio-oil composition and properties.

Literature Cited

(1) Antal, M. J.; Gronli, M. G. The art, science and technology of charcoal production. *Ind. Eng. Chem. Res.* **2003**, *42*, 1619.

(2) Bridgwater, A. V. Principles and practice of biomass fast pyrolysis processes for liquids. *J. Anal. Appl. Pyrolysis* **1999**, *51*, 3.

(3) Scott, D. S.; Majerski, P.; Piskorz, J.; Radlein. D. A second look at fast pyrolysis of biomass—The RTI process. *J. Anal. Appl. Pyrolysis* **1999**, *51*, 23.

(4) Czernik, S.; Bridgwater, A. V. Overview of application of biomass fast pyrolysis oil. *Energy Fuels* **2004**, *18*, 590.

(5) Chiaramonti, D.; Oasmaa, A.; Solantausta, Y. Power generation using fast pyrolysis liquids from biomass. *Renewable Sustainable Energy Rev.*, in press.

(6) Wornat, M. J.; Porter, B. G.; Yang, N. Y. C. Single droplet combustion of biomass pyrolysis oils. *Energy Fuels* **1994**, *8*, 1131.

(7) Shaddix, C. R.; Huey, S. P. Combustion characteristics of fast pyrolysis oils derived from hybrid poplar. In *Developments in Thermochemical Biomass Conversion*; Bridgwater, A. V., Ed.; CPL Press: Newbury, U.K., 1997; pp 1−23.

(8) Shaddix, C. R.; Tennison, P. J. Effects of char content and simple additives on biomass pyrolysis oil droplet combustion. In *Proceedings of the 27th Symposium on Combustion*; The Combustion Institute: Pittsburgh, 1998; pp 1131−1142.

(9) D'Alessio, J.; Lazzaro, M.; Massoli, P.; Moccia, V. Thermo-optical investigation of burning biomass pyrolysis oil droplets. In *Proceedings of*

the 27th Symposium on Combustion; The Combustion Institute: Pittsburgh, 1998; pp 1915−1922.

(10) Ghetti, P.; Ricca, L.; Angelini, L. Thermal analysis of biomass and corresponding pyrolysis products. *Fuel* **1996**, *75*, 565.

(11) Vitolo, S.; Seggiani, M.; Frediani, P.; Ambrosini, G.; Politi, L. Catalytic upgrading of pyrolytic oils to fuel over different zeolites. *Fuel* **1999**, *78*, 1147.

(12) Branca, C.; Di Blasi, C.; Russo, C. Devolatilization in the temperature range 300−600K of liquids derived from wood pyrolysis and gasification. *Fuel* **2005**, *84*, 37.

(13) Branca, C.; Di Blasi, C.; Elefante, R. Devolatilization and heterogeneous combustion of wood fast pyrolysis oils. *Ind. Eng. Chem. Res.* **2005**, *44*, 799.

(14) Conesa, J. A.; Marcilla, A.; Caballero, J. A.; Font, R. Comments on the validity and utility of the different methods for kinetic analysis of thermogravimetric data. *J. Anal. Appl. Pyrolysis* **2001**, *58*−*59*, 617.

(15) Oasmaa, A.; Meier, D. Analysis, characterization and test methods of fast pyrolysis liquids. In *Fast Pyrolysis of Biomass: A Handbook*, Vol. 2; Bridgwater, A. V., Ed.; CPL Press: Newbury, U.K., 2002; pp 1−23.

(16) Branca, C.; Giudicianni, P.; Di Blasi, C. GC/MS characterization of liquids generated from low-temperature pyrolysis of wood. *Ind. Eng. Chem. Res.* **2003**, *42*, 3190.

(17) Antal, M. J.; Varhegyi, G. Cellulose pyrolysis kinetics: The current state of knowledge. *Ind. Eng. Chem. Res.* **1995**, *34*, 703.

(18) Gronli, M. G.; Varhegyi, G.; Di Blasi, C. Thermogravimetric analysis and devolatilization kinetics of wood. *Ind. Eng. Chem. Res.* **2002**, *41*, 4201.

(19) Branca, C.; Albano, A.; Di Blasi, C. Critical evaluation of wood devolatilization mechanisms. *Thermochim. Acta* **2005**, *429*, 133.

(20) Branca, C.; Di Blasi, C.; Horacek, H. Analysis of the combustion kinetics and the thermal behavior of an intumescent system. *Ind. Eng. Chem. Res.* **2002**, *41*, 2104.

(21) Boroson, M. L.; Howard, J. B.; Longwell, J. P.; Peters, A. W. Products, yields and kinetics from the vapor phase cracking of wood pyrolysis tars. *AIChE J.* **1989**, *35*, 120.

(22) Shresta, D.; Cramer, S.; White, R. Time−temperature profile across a lumber section exposed to pyrolytic temperatures. *Fire Mater.* **1994**, *18*, 211.

(23) Bryden, K. M.; Ragland, K. W.; Rutlan, C. J. Modeling thermally thick pyrolysis of wood. *Biomass Bioenergy* **2002**, *22*, 41.

(24) Di Blasi, C.; Branca, C.; Sparano, S.; La Mantia, B. Drying characteristics of wood cylinders for conditions pertinent to fixed-bed countercurrent gasification. *Biomass Bioenergy* **2003**, *25*, 45.

(25) Di Blasi, C. Kinetics and modeling of biomass pyrolysis. In *Fast Pyrolysis of Biomass: A Handbook*, Vol. 3; Bridgwater, A. V., Ed.; CPL Press: Newbury, U.K., 2005; pp 121−146.

Received for review February 8, 2006
Revised manuscript received April 19, 2006
Accepted June 8, 2006

IE060161X